

Real space thermalization of locally driven quantum magnets

Ronald Melendrez,^{1,2} Bhaskar Mukherjee,³ Prakash Sharma,^{1,2} Arijeet Pal,³ and Hitesh J. Changlani^{1,2}

¹Department of Physics, Florida State University, Tallahassee, Florida 32306, USA

²National High Magnetic Field Laboratory, Tallahassee, Florida 32304, USA

³Department of Physics and Astronomy, University College London, Gower Street, London WC1E 6BT, United Kingdom

(Dated: December 29, 2022)

Thermalization and its breakdown in isolated systems has led to a deeper understanding of non-equilibrium quantum states and their dependence on initial conditions. This is prominently highlighted by the existence of quantum scars, special athermal states with an underlying effective superspin structure, embedded in an otherwise chaotic many-body spectrum. Spin XXZ models and their variants in one and higher dimension have been shown to host exact quantum scars, exhibiting perfect revivals of spin helix states that are realizable in synthetic and condensed matter systems. Motivated by these advances, we propose experimentally accessible local, time-dependent protocols to explore the spatial thermalization profile and highlight how different parts of the system thermalize and affect the fate of the superspin. We identify distinct parametric regimes for the ferromagnetic (X -polarized) initial state based on the interplay between the driven spin and the rest, including local athermal behavior where the driven spin effectively decouples, acting like a “cold” spot while being instrumental in heating up the other spins. We develop a real and Floquet space picture that explains our numerical observations, and make predictions that can be tested in various experimental setups.

In a set of pioneering papers [1–4] the question of thermalization of isolated quantum systems was posed sharply and addressed. It is now understood that generic isolated quantum systems satisfy the eigenstate thermalization hypothesis. Broadly said, local observables are insensitive to the choice of eigenstate at a given energy density and the system is “self-thermal” i.e. it acts as its own heat bath. However, there are important exceptions, among them “emergent integrable” systems e.g. many-body localized systems [5–9] and systems which are “partially integrable” or those with “quantum scars”. [10–13] The search for quantum scars, athermal states embedded in the spectra of otherwise chaotic systems, has seen recent activity [12–35] because of fundamental interest and due to proposals for using them for quantum sensing [34, 36]. Scar states frequently occur when the Hilbert space is fragmented due to kinetic constraints [23, 37–40]. In a time-dependent setting, the presence of a global periodic drive can either destabilize or stabilize athermal behaviour [41, 42] - e.g. under certain conditions it can exhibit slow thermalization and dynamical freezing [43].

In previous work, some of us identified the XXZ model as a simple platform for realizing quantum scars and Hilbert-space fragmentation (HSF) [22, 23]. The model shares a common unifying theme with other models of scars (including the widely studied PXP one [13, 44]) - there is a “superspin” whose precession is responsible for revivals in various numerically computed and experimentally measured physical observables. Such a superspin can be realized as the ferromagnetic state in the middle of the energy spectrum (the exact $SU(2)$ degeneracy being split by a magnetic field) by “staggering” the XXZ model i.e. by alternating the sign of interaction on even/odd bonds (or more generally on different motifs) [22]. When the spins are prepared in a collective coherent state (e.g. in the all $X \equiv \Pi_i \otimes | \rightarrow \rangle_i$ state) their dynamics corresponds to that of a superspin.

But how do such scars thermalize when subjected to time-

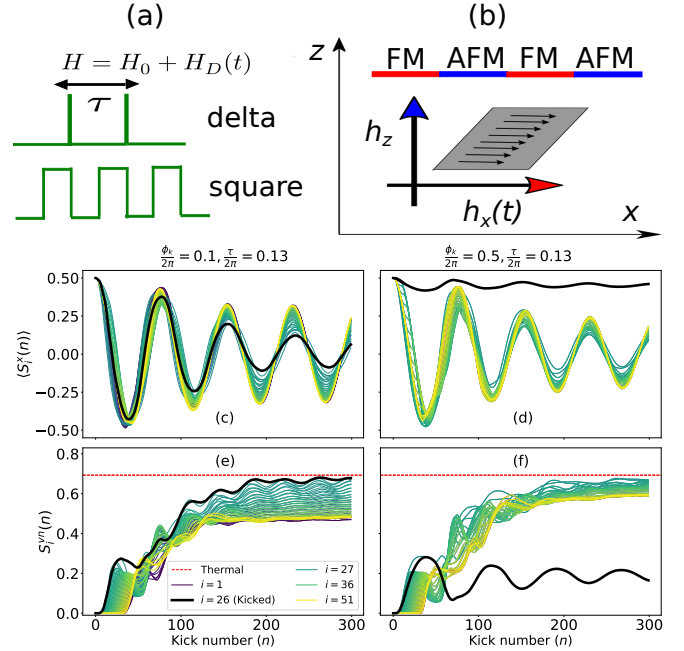


FIG. 1. Schematic of (a) Local kick protocols and (b) the system studied in this work. The alternating (staggered) interactions place the ferromagnetic state in the middle of the spectrum. For the local delta kick we show two characteristic behaviors for a $N = 51$ site system with open boundary conditions with the kick at the central site (c,d) show $\langle S_i^x \rangle$ and (e,f) the Von-Neumann entanglement entropy of representative sites. Results are for $\tau/2\pi = 0.13$ and (c,e) $\phi_k/2\pi = 0.1$ and (d,f) $\phi_k/2\pi = 0.5$. For the case of weak kick, the driven site thermalizes, for stronger kicks it remains athermal.

dependent fields? Our motivation for answering this stems from expanding the existing dichotomy of classifying a system as thermalized vs athermal - after all, could it be that there are parts of the system that are athermal while the rest have thermalized? We explore this question in the context of a periodic, local drive [45–47], and demonstrate the crossover

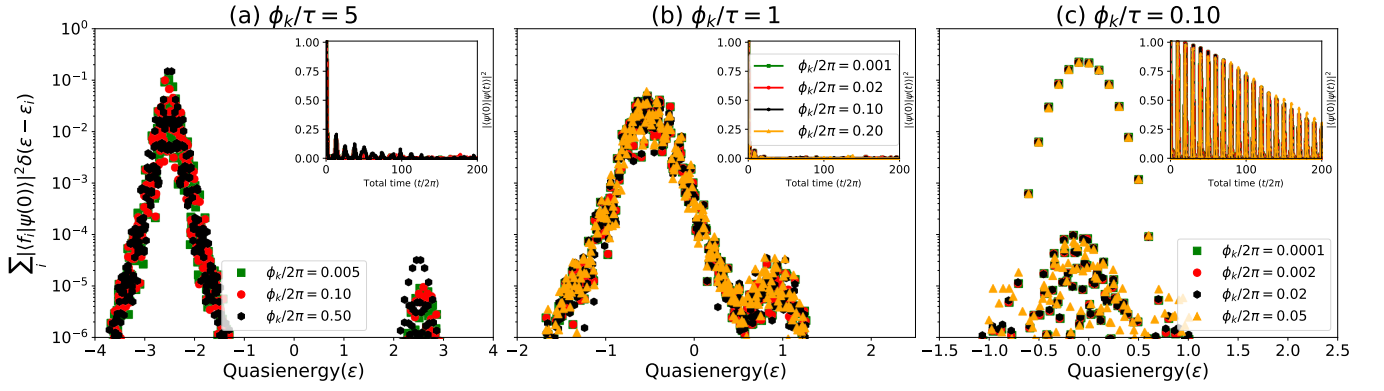


FIG. 2. Floquet overlap profile and (inset) survival probability/Loschmidt echo starting from the fully polarized X state, for representative cases of the local delta kick protocol for $N = 12$ sites with periodic boundary conditions (a) $\phi_k/\tau = 5$ (b) $\phi_k/\tau = 1$ and (c) $\phi_k/\tau = 0.1$. For ease of visualization (and to account for situations with near or exact degeneracies), quasienergies are binned with a spacing of 10^{-2} , and the total overlap on the (nearly) degenerate manifold is reported.

between regimes of weak HSF and quantum scarring where the system locally remains prethermal due to the interplay between the dynamics of the driven spin with the rest of the system. We investigate two time-dependent potentials, schematically depicted in Fig. 1, whose similarities and differences we highlight especially in the context of the effective Floquet Hamiltonian they realize. In both cases the Hamiltonian is given by $H = H_0 + H_D(t)$ where,

$$H_0 \equiv J \sum_i (-1)^i \vec{S}_i \cdot \vec{S}_{i+1} - h \sum_i S_i^z \quad (1)$$

J (set to 1 throughout) is the alternating (staggered) ferro- and antiferromagnetic interaction strength, h is the strength of the magnetic (Zeeman) field, and i is a site index, $i + 1$ is taken modulo N for periodic boundary conditions. (For open boundary conditions the bond to the $(N + 1)^{th}$ spin does not exist and is not counted). We note that study of H_0 , primarily in the context of its ground state properties, has a long history due to its relevance to Haldane spin chains [48–50].

In the first “delta kick” protocol, we have,

$$H_D(t) \equiv - \sum_{n>0} \sum_i \phi_i S_i^x \delta(t - n\tau) \quad (2)$$

where ϕ_i denote the applied transverse field strengths local to site i . While there is a considerable amount of work on models where a collective spin is kicked [51–53]), we emphasize that H here has only local interactions, and the system behaves as a collective spin degree of freedom only for certain initial conditions. In practice, the delta kick is just an approximation to a transverse field pulse applied for a time much shorter than the time between two such pulses. Here we focus on ϕ_k non-zero (a kick applied at the k -th site) and the rest zero.

The second protocol is that of a symmetric square pulse i.e. the transverse field has opposite sign for $[0, \tau/2]$ and $[\tau/2, \tau]$ and is periodic,

$$H_D(t) \equiv \sum_i \gamma_i \text{Sgn}\left(\sin\left(\frac{2\pi t}{\tau}\right)\right) S_i^x \quad (3)$$

A similar drive pulse protocol (but with different H_0) was considered recently for global drives in the context of conditions for resonant scars [43]. Here we consider the case of γ_k non zero on the driven site and the rest zero. For both the delta kick and square pulse protocols, we have identified regimes where the driven spin either collectively thermalizes with the rest of the spins (as shown in Fig. 1 (c,e)) or essentially disentangles itself from the remainder of the spins (Fig. 1(d,f)). The latter case serves as an example of a system that is locally kept athermal (or “cold”) by driving whereas the rest of the system “heats up” and thermalizes.

Floquet and real space pictures: We discuss both the Floquet (“quasienergy”) space and local (real space) picture of this phenomenon by first placing its behavior in the context of a familiar picture of quantum scars. The Floquet spectrum now assumes the role of eigenenergies of the (time independent) Hamiltonian where identification of an isolated manifold with large overlap on the initial state revealed the existence of scars. For stroboscopic times the unitary Floquet operator encodes the time evolution, which for a single period is given by $F(\tau) \equiv e^{-iH_F\tau} = \sum_j e^{-i\epsilon_j\tau} |f_j\rangle\langle f_j|$ with H_F the effective Hermitian “Floquet Hamiltonian”, $|f_j\rangle$ the j^{th} Floquet eigenvector and ϵ_j is the corresponding quasienergy. For our two drive protocols we have,

$$F(\tau) = e^{+i \sum_i \phi_i S_i^x} e^{-iH_0\tau} \quad \text{delta} \quad (4)$$

$$F(\tau) = e^{-i(H_0 - \sum_i \gamma_i S_i^x) \frac{\tau}{2}} e^{-i(H_0 + \sum_i \gamma_i S_i^x) \frac{\tau}{2}} \quad \text{square} \quad (5)$$

Knowing f_j and ϵ_j and hence $c_j \equiv \langle f_j | \psi(0) \rangle$, one can infer many properties of the dynamics, for example, the survival probability (Loschmidt echo) is $|\langle \psi(0) | \psi(n\tau) \rangle|^2 = \sum_{j,k} |c_j|^2 |c_k|^2 e^{-in(\epsilon_j - \epsilon_k)\tau}$ and since the quasienergies typically have more or less random spacings, it goes to zero by virtue of the superposition of the (almost) random phases. However, this is not always the case - a regularity in states with dominant $|c_i|$ leads to robust revivals of the survival probability (and other observables). We thus plot c_j as a function of ϵ_j and refer to it as the “Floquet overlap profile” as in

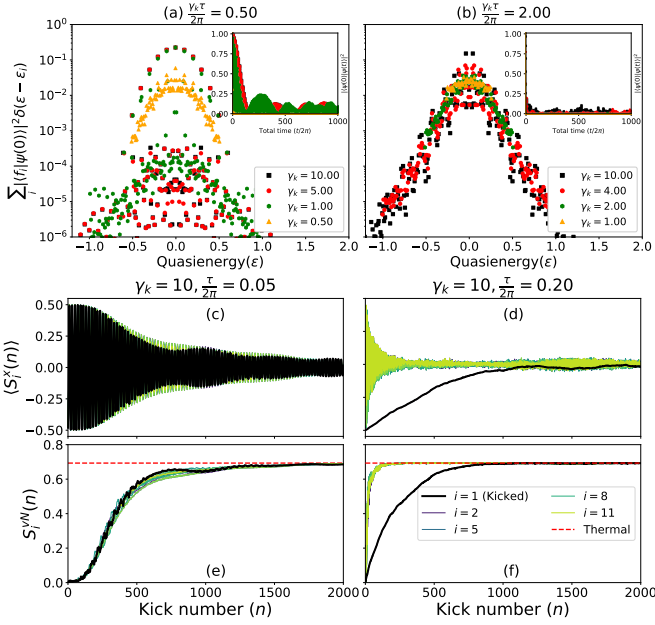


FIG. 3. (a,b) Floquet overlap profile and (inset) survival probability/Loschmidt echo starting from the X state, for representative parameters of the local square pulse protocol for $N = 12$ sites with periodic boundary conditions. $\gamma_k \tau / 2\pi$ was fixed to the value of (a) 0.50 and (b) 2, while individually varying γ_k and τ . The value in (b) satisfies the resonant condition, see text. Quasienergies are binned with a spacing of 10^{-2} , and the total overlap on the (nearly) degenerate manifold is reported. Panels (c,d) show $\langle S_i^x(t) \rangle$ and panels (e,f) show the Von-Neumann entanglement entropy $S_i^{vN}(t)$ for all sites (i) for the cases of (c,e) $\gamma_k = 10, \tau/2\pi = 0.05$ and (d,f) $\gamma_k = 10, \tau/2\pi = 0.20$. The left panels (c,e) show that a single site drive is sufficient to thermalize all the sites. The right panels (d,f) show slow relaxation of local properties at the driven site due to the resonant condition obtained from $H_F^{(0)}$.

Figs. 2 and 3.

Consider first the case of the local delta kick. On performing a BCH expansion of Eq. 4, the Floquet Hamiltonian to lowest order is shown to be $H_F = H_0 - \frac{\phi_k}{\tau} S_k^x$ (see SM). This suggests that the Floquet overlap profile and survival probability must be approximately a function of ϕ_k/τ , the fact that our data collapse onto each other (for weak ϕ_k) show that this is indeed the case. (This collapse breaks down for larger ϕ_k since there are higher order terms in the Floquet Hamil-

tonian, see SM. Also $\phi_k = 2n\pi$ is special and corresponds to the situation where there is no kick). When ϕ_k/τ is large, the Floquet quasienergies are $+\phi_k/2\tau$ and $-\phi_k/2\tau$, half the Floquet eigenvectors have $S_k^x = 1/2$ and the other half have $S_k^x = -1/2$. Strictly speaking, S_k^x is not an exact integral of motion for finite $\phi_k/2\tau$, this is a realization of weak HSF, the system is divided into two weakly coupled fragments in Hilbert space. The X state to overlap only onto the manifold of states with $S_k^x = 1/2$. On lowering ϕ_k/τ the X state begins to have overlap with both values of S_k^x , the Floquet overlap profile now broadens around the “bands” at $\pm\phi_k/2\tau$. When these bands do not overlap (as in Fig. 2(a) corresponding to $\phi_k/\tau = 5$) the kicked spin is athermal. The survival probability (in the inset) does not show any prominent oscillations, and since it is a global property it does not capture the lack of thermalization of the driven spin. The lack of any regular structure in the Floquet overlap profile is ultimately at the heart of thermalization of the undriven spins.

On weakening ϕ_k/τ , the isolated Floquet “bands” broaden and eventually begin to merge with one another. When this happens, the driven spin does not act significantly differently from the rest of the spins. The notion of this collective thermalization is corroborated in Fig. 1. When the local delta kick is weakened even further, a long thermalization scale emerges due to the vicinity to a “perfect scar” since the X state is in the null space of the staggered Heisenberg term - it has a decomposition onto the tower of $2(N/2) + 1$ states. The Floquet overlap profile for $\phi_k/\tau = 0.1$ demonstrates this very clearly, the quasienergy spacing between states with non-zero overlap is h arising from the Zeeman splitting of the embedded ferromagnet. (The limit $\phi_k \rightarrow 0$ corresponds to the undriven case i.e. $H_F = H_0$.)

The Floquet framework (coupled with either the BCH expansion of the participating operators or the Floquet-Magnus expansion) offers a way to understand (and hence engineer) the lifetime of the scar like state. For example, consider a driven spin with a kick that alternates in sign - in the limit of high frequency the kicks of opposite sign “effectively cancel out” and the system is essentially undriven (to lowest order). The “symmetric” square pulse we consider next also satisfies this criterion. As shown in the SM, the Floquet Hamiltonian for the local square pulse to lowest order is,

$$\begin{aligned}
H_F^{(0)} = & (-1)^k [S_k^x S_{k+1}^x + \frac{2 \sin(\frac{\gamma_k \tau}{2})}{\gamma_k \tau} (S_k^y S_{k+1}^y + S_k^z S_{k+1}^z) - \frac{2(1 - \cos(\frac{\gamma_k \tau}{2}))}{\gamma_k \tau} (S_k^z S_{k+1}^y - S_k^y S_{k+1}^z)] \\
& - (-1)^k [S_{k-1}^x S_k^x + \frac{2 \sin(\frac{\gamma_k \tau}{2})}{\gamma_k \tau} (S_{k-1}^y S_k^y + S_{k-1}^z S_k^z) - \frac{2(1 - \cos(\frac{\gamma_k \tau}{2}))}{\gamma_k \tau} (S_{k-1}^z S_k^y - S_{k-1}^y S_k^z)] \\
& - \frac{2h}{\gamma_k \tau} (\sin(\frac{\gamma_k \tau}{2}) S_k^z + (1 - \cos(\frac{\gamma_k \tau}{2})) S_k^y) + \sum_{\substack{i=1 \\ i \neq (k-1, k)}}^{N-1} (-1)^i S_i \cdot S_{i+1} - h \sum_{\substack{i=1 \\ i \neq k}}^N S_i^z
\end{aligned} \tag{6}$$

Two important takeaways are (1) $H_F^{(0)}$ just depends on $\gamma_k \tau$,

a finding confirmed by the collapse seen in the Floquet over-

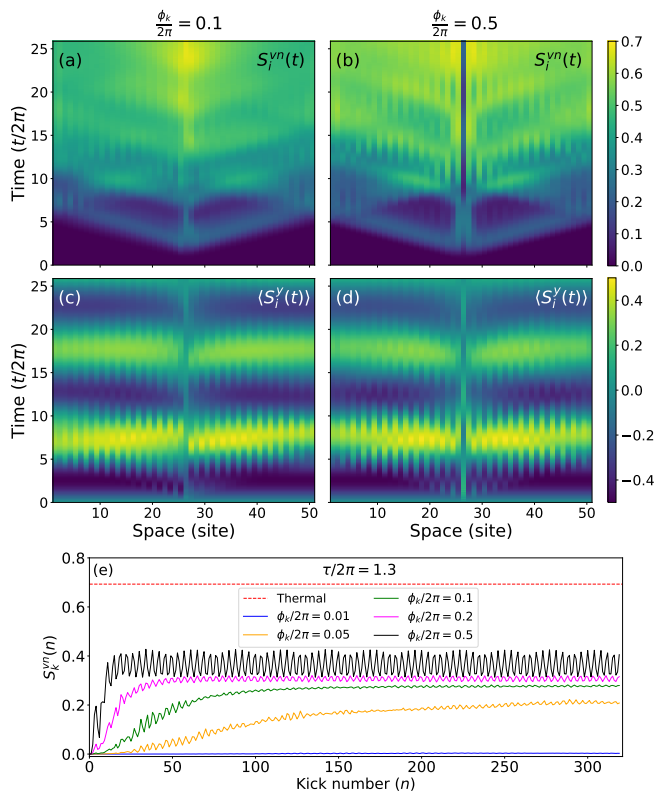


FIG. 4. Space-time thermalization profile for a $N = 51$ site delta kicked staggered XXZ chain with open boundary conditions, showing the Von-Neumann entanglement entropy (a,b) $S_i^{vN}(t)$ of each site and (c,d) $\langle S_i^y(t) \rangle$. Space and time correspond to the horizontal and vertical axes respectively and the color represents the value of the physical quantity. Results are shown for $\tau/2\pi = 0.13$ and (a,c) $\phi_k/2\pi = 0.1$ and (b,d) $\phi_k/2\pi = 0.5$. (e) The Von-Neumann entanglement entropy of the kicked site for the case of $\tau/2\pi = 1.3$ and a few representative values of ϕ_k .

lap profile in Fig. 3 (a,b) and (2) there are special values of drive frequency and strength - the so called “resonant condition” ($\gamma_k = 4\pi n/\tau$) where the system is locally athermal, a phenomenon referred to as dynamic freezing. Since the F-M expansion is most accurate at high drive frequency ($1/\tau \gg 1$), we expect the Floquet Hamiltonian to be well approximated by H_F^0 only in those regimes.

At extremely high frequencies, the drive is rendered ineffective leading to oscillations starting from the X -polarized state (not shown). At intermediate frequencies, single site driving is sufficient to thermalize all the sites including the driven site (see Fig. 3(c,e)), reminiscent of the behavior of the delta kicked system for intermediate ϕ_k/τ . At the resonant frequencies however, unlike the case of global drive [43], the driven spin is not entirely frozen out, but does relax slowly compared to the others (see Fig. 3(d,f)). This ruining of dynamic freezing is caused by higher order terms in the F-M expansion of H_F . (We will present further subtleties elsewhere.)

Real-space, real-time profile of thermalization. We now take a more refined look at the real-space, real-time picture of thermalization for an open chain where the central site is sub-

ject to a periodic delta kick. In Fig. 4 we construct a space-time plot of the Von-Neumann entanglement entropy of the site and the onsite expectation value of S_i^y . The calculations were done with the matrix product state based time evolution block decimation algorithm [54] on a $N = 51$ site system with open boundary conditions with a maximum bond dimension of 400.

Since the system is initially prepared in the X state, the entanglement of each spin is exactly zero to begin with. As time progresses, the entanglement spreads out in a “cone”, distant regions begin to feel the kick as time progresses and the cone reaches the edges of the system. This can be seen prominently for $\tau/2\pi = 0.13$ for both $\phi_k/2\pi = 0.1$ and $\phi_k/2\pi = 0.5$ at short times. After this initial phase, the regions around the central spin show a prominent dip in their entanglement (i.e. they get cold after an initial phase of heating up), this appears as two blue lobes around the kicked spin, as time progresses these regions heat up. (Note that the system is not inversion symmetric because of the alternating J 's, but approximately appears to be so for the entanglement entropy). The entire plot shows oscillatory behavior both in space and time, similar observations although for a different model and observables have been reported recently in Ref. [55]. On the time scale of the plot $\langle S_i^y \rangle$ appears to show robust collective revivals (which eventually do decay), however the central driven spin shows weakened oscillations. These oscillations, at short times, are largely in phase with the other spins for $\phi_k/2\pi = 0.1$, but out of phase for $\phi_k/2\pi = 0.5$.

Finally, we consider the case of effectively weaker kicks by fixing the kick frequency to a value 10 times smaller i.e. $\tau/2\pi = 1.3$ and a few representative values of ϕ_k in Fig. 4 (e). After an initial stage of entanglement growth, we see entanglement oscillations for the kicked spin (and other spins, not shown) which remain robust and oscillate about a non zero value. The value of this plateau and the strength of the oscillations both grow with ϕ_k . The fact that this value is far from the thermal expectation of $\ln 2$, and that its value is similar for all spins, suggests that despite the breaking of translational symmetry, the superspin picture is intact after the information from the kicked site has reached the boundaries of the system. This reflects the resilience of the superspin to local driving. On the time scale of our TEBD simulations we can not determine if this is truly athermal or prethermal behavior. We must clarify though that the existence of finite entanglement for every site is considerably different from the limit of no kick where the system always remains in a product state during the time evolution - one can simply think of the interactions as ineffective due to the choice of initial condition. However, in the weakly driven case the system appears to have self-organized itself (after an initial period of entanglement growth) to collectively remain as a superspin.

Outlook. In summary, we have explored the different dynamic regimes of a locally driven XXZ spin chain hosting exact quantum scars for drive protocols that should be experimentally accessible. For the X -polarized initial state, which shows perfect revivals for the time-independent case,

the driven spin crosses over from full thermalization to athermal dynamics, effectively decoupling from the rest of the spins, as the rest of the system thermalizes. Both our protocols showed the existence of an effectively decoupled spin, however the origin of this effect was different for the delta and square pulses, which we highlighted in the text. We believe these predictions can be tested - there are now many synthetic realizations of spin systems: in addition to Rydberg atoms, ytterbium-171 has been recently used to realize an effective transverse Ising model [56] and hyperfine states of lithium realize XXZ models with tunable anisotropy [57]. Our observation of the local breakdown of thermalization in an otherwise thermal system for a certain initial state provides a non-trivial mechanism for protecting information in a periodically driven system and sheds light on the novel behaviour of dynamics of many-body entanglement.

Acknowledgements: We thank Kyungmin Lee for useful discussions in the initial stages of the project and for a previous collaboration. R.M., P.S. and H.J.C. acknowledge support from Grant No. NSF DMR- 2046570 and Florida State University (FSU) and the National High Magnetic Field Laboratory. The National High Magnetic Field Laboratory is supported by the National Science Foundation through Grant No. DMR-1644779 and by the state of Florida. A.P. and B. M. were funded by the European Research Council (ERC) under the European Union’s Horizon 2020 research and innovation programme (Grant Agreement No. 853368). We also thank the Planck cluster and the Research Computing Center (RCC) at FSU for computing resources. The MPS based TEBD calculations were based on the ITensor library [58]

Note added: During the preparation of this work, we became aware of arXiv:2211.00040 which realizes cold and hot regions in a driven system.

-
- [1] J. M. Deutsch, “Quantum statistical mechanics in a closed system,” *Phys. Rev. A* **43**, 2046 (1991).
- [2] Mark Srednicki, “Chaos and quantum thermalization,” *Phys. Rev. E* **50**, 888 (1994).
- [3] Marcos Rigol, Vanja Dunjko, and Maxim Olshanii, “Thermalization and its mechanism for generic isolated quantum systems,” *Nature (London)* **452**, 854 (2008).
- [4] R. V. Jensen and R. Shankar, “Statistical behavior in deterministic quantum systems with few degrees of freedom,” *Phys. Rev. Lett.* **54**, 1879–1882 (1985).
- [5] D. M. Basko, I. L. Aleiner, and B. L. Altshuler, “Metal-insulator transition in a weakly interacting many-electron system with localized single-particle states,” *Ann. Phys. (N.Y.)* **321**, 1126 (2006).
- [6] Arijeet Pal and David A. Huse, “Many-body localization phase transition,” *Phys. Rev. B* **82**, 174411 (2010).
- [7] Vadim Oganesyan and David A. Huse, “Localization of interacting fermions at high temperature,” *Phys. Rev. B* **75**, 155111 (2007).
- [8] Rahul Nandkishore and David A. Huse, “Many-body localization and thermalization in quantum statistical mechanics,” *Annu. Rev. Condens. Matter Phys.* **6**, 15–38 (2015).
- [9] Dmitry A. Abanin, Ehud Altman, Immanuel Bloch, and Maksym Serbyn, “Colloquium: Many-body localization, thermalization, and entanglement,” *Rev. Mod. Phys.* **91**, 021001 (2019).
- [10] Eric J. Heller, “Bound-state eigenfunctions of classically chaotic Hamiltonian systems: Scars of periodic orbits,” *Phys. Rev. Lett.* **53**, 1515 (1984).
- [11] Oskar Vafek, Nicolas Regnault, and B. Andrei Bernevig, “Entanglement of exact excited eigenstates of the Hubbard model in arbitrary dimension,” *SciPost Phys.* **3**, 043 (2017).
- [12] Naoto Shiraishi and Takashi Mori, “Systematic construction of counterexamples to the eigenstate thermalization hypothesis,” *Phys. Rev. Lett.* **119**, 030601 (2017).
- [13] C. J. Turner, A. A. Michailidis, D. A. Abanin, M. Serbyn, and Z. Papić, “Weak ergodicity breaking from quantum many-body scars,” *Nat. Phys.* **14**, 745 (2018).
- [14] C. J. Turner, A. A. Michailidis, D. A. Abanin, M. Serbyn, and Z. Papić, “Quantum scarred eigenstates in a Rydberg atom chain: Entanglement, breakdown of thermalization, and stability to perturbations,” *Phys. Rev. B* **98**, 155134 (2018).
- [15] Sanjay Moudgalya, Stephan Rachel, B. Andrei Bernevig, and Nicolas Regnault, “Exact excited states of nonintegrable models,” *Phys. Rev. B* **98**, 235155 (2018).
- [16] Sanjay Moudgalya, Nicolas Regnault, and B. Andrei Bernevig, “Entanglement of exact excited states of Affleck-Kennedy-Lieb-Tasaki models: Exact results, many-body scars, and violation of the strong eigenstate thermalization hypothesis,” *Phys. Rev. B* **98**, 235156 (2018).
- [17] Cheng-Ju Lin and Olexei I. Motrunich, “Exact quantum many-body scar states in the Rydberg-blockaded atom chain,” *Phys. Rev. Lett.* **122**, 173401 (2019).
- [18] Vedika Khemani, Chris R. Laumann, and Anushya Chandran, “Signatures of integrability in the dynamics of Rydberg-blockaded chains,” *Phys. Rev. B* **99**, 161101(R) (2019).
- [19] Kieran Bull, Ivar Martin, and Z. Papić, “Systematic construction of scarred many-body dynamics in 1D lattice models,” *Phys. Rev. Lett.* **123**, 030601 (2019).
- [20] Michael Schecter and Thomas Iadecola, “Weak ergodicity breaking and quantum many-body scars in spin-1 XY magnets,” *Phys. Rev. Lett.* **123**, 147201 (2019).
- [21] Seulgi Ok, Kenny Choo, Christopher Mudry, Claudio Castellano, Claudio Chamon, and Titus Neupert, “Topological many-body scar states in dimensions one, two, and three,” *Phys. Rev. Research* **1**, 033144 (2019).
- [22] Kyungmin Lee, Ronald Melendrez, Arijeet Pal, and Hitesh J. Changlani, “Exact three-colored quantum scars from geometric frustration,” *Phys. Rev. B* **101**, 241111 (2020).
- [23] Kyungmin Lee, Arijeet Pal, and Hitesh J. Changlani, “Frustration-induced emergent hilbert space fragmentation,” *Phys. Rev. B* **103**, 235133 (2021).
- [24] Paul A. McClarty, Masudul Haque, Arnab Sen, and Johannes Richter, “Disorder-free localization and many-body quantum scars from magnetic frustration,” *Phys. Rev. B* **102**, 224303 (2020).
- [25] Julia Wildeboer, Alexander Seidel, N. S. Srivatsa, Anne E. B. Nielsen, and Onur Erten, “Topological quantum many-body scars in quantum dimer models on the kagome lattice,” *Phys. Rev. B* **104**, L121103 (2021).
- [26] K. Pakrouski, P. N. Pallegar, F. K. Popov, and I. R. Klebanov, “Many-body scars as a group invariant sector of hilbert space,” *Phys. Rev. Lett.* **125**, 230602 (2020).
- [27] Bart van Voorden, Jiří Minář, and Kareljan Schoutens, “Quantum many-body scars in transverse field ising ladders and beyond,” *Phys. Rev. B* **101**, 220305 (2020).

- [28] Wen-Long You, Zhuan Zhao, Jie Ren, Gaoyong Sun, Liangsheng Li, and Andrzej M. Oleś, “Quantum many-body scars in spin-1 kitaev chains,” *Phys. Rev. Research* **4**, 013103 (2022).
- [29] Eli Chertkov and Bryan K. Clark, “Motif magnetism and quantum many-body scars,” *Phys. Rev. B* **104**, 104410 (2021).
- [30] Yoshihito Kuno, Tomonari Mizoguchi, and Yasuhiro Hatsugai, “Flat band quantum scar,” *Phys. Rev. B* **102**, 241115 (2020).
- [31] E. S. Ma, K. L. Zhang, and Z. Song, “Steady helix states in a resonant xxz heisenberg model with dzyaloshinskii-moriya interaction,” *Phys. Rev. B* **106**, 245122 (2022).
- [32] Prakash Sharma, Kyungmin Lee, and Hitesh J. Changlani, “Multimagnon dynamics and thermalization in the $s = 1$ easy-axis ferromagnetic chain,” *Phys. Rev. B* **105**, 054413 (2022).
- [33] Saül Pilatowsky-Cameo, David Villaseñor, Miguel A. Bastarrachea-Magnani, Sergio Lerma-Hernández, Lea F. Santos, and Jorge G. Hirsch, “Ubiquitous quantum scarring does not prevent ergodicity,” *Nature Communications* **12**, 852 (2021).
- [34] Maksym Serbyn, Dmitry A. Abanin, and Zlatko Papić, “Quantum many-body scars and weak breaking of ergodicity,” (2020), [arXiv:2011.09486 \[quant-ph\]](https://arxiv.org/abs/2011.09486).
- [35] Anushya Chandran, Thomas Iadecola, Vedika Khemani, and Roderich Moessner, “Quantum many-body scars: A quasiparticle perspective,” (2022).
- [36] Shane Dooley, “Robust quantum sensing in strongly interacting systems with many-body scars,” *PRX Quantum* **2**, 020330 (2021).
- [37] Pablo Sala, Tibor Rakovszky, Ruben Verresen, Michael Knap, and Frank Pollmann, “Ergodicity breaking arising from Hilbert space fragmentation in dipole-conserving Hamiltonians,” *Phys. Rev. X* **10**, 011047 (2020).
- [38] Vedika Khemani, Michael Hermele, and Rahul Nandkishore, “Localization from Hilbert space shattering: From theory to physical realizations,” *Phys. Rev. B* **101**, 174204 (2020).
- [39] Alexey Khudorozhkov, Apoorv Tiwari, Claudio Chamon, and Titus Neupert, “Hilbert space fragmentation in a 2D quantum spin system with subsystem symmetries,” *SciPost Phys.* **13**, 098 (2022).
- [40] Sanjay Moudgalya and Olexei I. Motrunich, “Hilbert space fragmentation and commutant algebras,” *Phys. Rev. X* **12**, 011050 (2022).
- [41] Bhaskar Mukherjee, Sourav Nandy, Arnab Sen, Diptiman Sen, and K. Sengupta, “Collapse and revival of quantum many-body scars via floquet engineering,” *Phys. Rev. B* **101**, 245107 (2020).
- [42] D. Bluvstein, A. Omran, H. Levine, A. Keesling, G. Semeghini, S. Ebadi, T. T. Wang, A. A. Michailidis, N. Maskara, W. W. Ho, and et al., “Controlling quantum many-body dynamics in driven rydberg atom arrays,” *Science* **371**, 1355–1359 (2021).
- [43] Asmi Haldar, Diptiman Sen, Roderich Moessner, and Arnab Das, “Dynamical freezing and scar points in strongly driven floquet matter: Resonance vs emergent conservation laws,” *Phys. Rev. X* **11**, 021008 (2021).
- [44] C. J. Turner, A. A. Michailidis, D. A. Abanin, M. Serbyn, and Z. Papić, “Weak ergodicity breaking from quantum many-body scars,” *Nature Physics* **14**, 745–749 (2018).
- [45] Daniel Thuberg, Sebastián A. Reyes, and Sebastian Eggert, “Quantum resonance catastrophe for conductance through a periodically driven barrier,” *Phys. Rev. B* **93**, 180301 (2016).
- [46] Adhip Agarwala and Diptiman Sen, “Effects of local periodic driving on transport and generation of bound states,” *Phys. Rev. B* **96**, 104309 (2017).
- [47] Friedrich Hübner, Christoph Dauer, Sebastian Eggert, Corinna Kollath, and Ameneh Sheikhan, “Floquet-engineered pair and single-particle filters in the fermi-hubbard model,” *Phys. Rev. A* **106**, 043303 (2022).
- [48] F. D. M. Haldane, “Nonlinear field theory of large-spin heisenberg antiferromagnets: Semiclassically quantized solitons of the one-dimensional easy-axis néel state,” *Phys. Rev. Lett.* **50**, 1153–1156 (1983).
- [49] Kazuo Hida, “Crossover between the haldane-gap phase and the dimer phase in the spin-1/2 alternating heisenberg chain,” *Phys. Rev. B* **45**, 2207–2212 (1992).
- [50] Mahito Kohmoto and Hal Tasaki, “Hidden $z_2 \times z_2$ symmetry breaking and the haldane phase in the $s=1/2$ quantum spin chain with bond alternation,” *Phys. Rev. B* **46**, 3486–3495 (1992).
- [51] Ph. Jacquod, P.G. Silvestrov, and C.W.J. Beenakker, “Golden rule decay versus lyapunov decay of the quantum loschmidt echo,” *Phys. Rev. E* **64**, 055203 (2001).
- [52] Fritz Haake, M Kuś, and Rainer Scharf, “Classical and quantum chaos for a kicked top,” *Zeitschrift für Physik B Condensed Matter* **65**, 381–395 (1987).
- [53] Sudip Sinha, Sayak Ray, and Subhasis Sinha, “Fingerprint of chaos and quantum scars in kicked dicke model: an out-of-time-order correlator study,” *Journal of Physics: Condensed Matter* **33**, 174005 (2021).
- [54] Guifré Vidal, “Efficient classical simulation of slightly entangled quantum computations,” *Physical Review Letters* **91** (2003), [10.1103/physrevlett.91.147902](https://arxiv.org/abs/10.1103/physrevlett.91.147902).
- [55] Dong Yuan, Shun-Yao Zhang, Yu Wang, L.-M. Duan, and Dong-Ling Deng, “Quantum information scrambling in quantum many-body scarred systems,” *Phys. Rev. Res.* **4**, 023095 (2022).
- [56] W. L. Tan, P. Becker, F. Liu, G. Pagano, K. S. Collins, A. De, L. Feng, H. B. Kaplan, A. Kyprianidis, R. Lundgren, W. Morong, S. Whitsitt, A. V. Gorshkov, and C. Monroe, “Domain-wall confinement and dynamics in a quantum simulator,” *Nature Physics* **17**, 742–747 (2021).
- [57] Paul Niklas Jepsen, Yoo Kyung ‘Eunice’ Lee, Hanzhen Lin, Ivana Dimitrova, Yair Margalit, Wen Wei Ho, and Wolfgang Ketterle, “Long-lived phantom helix states in heisenberg quantum magnets,” *Nature Physics* **18**, 899–904 (2022).
- [58] Matthew Fishman, Steven R. White, and E. Miles Stoudenmire, “The ITensor software library for tensor network calculations,” (2020), [arXiv:2007.14822](https://arxiv.org/abs/2007.14822).
- [59] “Analytic approaches to periodically driven closed quantum systems: methods and applications,” *Journal of Physics: Condensed Matter* **33** (2021), [10.1088/1361-648X/ac1b61](https://doi.org/10.1088/1361-648X/ac1b61).
- [60] Szabolcs Vajna, Katja Klobas, Tomaž Prosen, and Anatoli Polkovnikov, “Replica resummation of the baker-campbell-hausdorff series,” *Phys. Rev. Lett.* **120**, 200607 (2018).
- [61] Marin Bukov, Luca D’Alessio, and Anatoli Polkovnikov, “Universal high-frequency behavior of periodically driven systems: from dynamical stabilization to floquet engineering,” *Advances in Physics* **64**, 139–226 (2015), <https://doi.org/10.1080/00018732.2015.1055918>.
- [62] Luca D’Alessio and Anatoli Polkovnikov, “Many-body energy localization transition in periodically driven systems,” *Annals of Physics* **333**, 19–33 (2013).

Supplemental Material for “Real space thermalization of locally driven quantum magnets”

In this supplemental material we provide a detailed calculation of the Floquet effective Hamiltonian (H_F) for both the periodic delta kick and square pulse protocol.

H_F FOR THE PERIODIC DELTA KICK PROTOCOL

Here we obtain the Floquet effective Hamiltonian (H_F) for periodic delta kick protocol using the truncated BCH expansion. Note that H_F for the kicked protocol is given by,

$$e^{-iH_F\tau} = e^{i\phi_k S_k^x} e^{-iH_0\tau} \quad (S1)$$

Set $X \equiv i\phi_k S_k^x$, $Y \equiv -iH_0\tau$ and $Z \equiv -iH_F\tau$, then H_F is given by

$$\begin{aligned} H_F &= \frac{iZ}{\tau} \\ &= \frac{i}{\tau} \ln(e^X e^Y) \\ &= H_F^{(0)} + H_F^{(1)} + H_F^{(2)} + \dots \end{aligned} \quad (S2)$$

where $H_F^{(n)}$ s can be determined using the BCH formula,

$$\begin{aligned} H_F^{(0)} &= \frac{i}{\tau} (X + Y) = H_0 - \frac{\phi_k}{\tau} S_k^x \\ H_F^{(1)} &= \frac{i}{\tau} \frac{[X, Y]}{2} = \frac{\phi_k}{2} (S_{k-1}^y S_k^z + S_k^y S_{k+1}^z - S_{k-1}^z S_k^y - S_k^z S_{k+1}^y - h S_k^y) \end{aligned} \quad (S3)$$

H_F FOR THE SQUARE PULSE PROTOCOL

Here we provide a detailed calculation of stroboscopic Floquet effective Hamiltonian (H_F) for the square pulse protocol using the Floquet-Magnus (F-M) expansion in a rotating frame. The F-M method yields H_F as a perturbative expansion in inverse drive frequency (τ). However, transition to a rotating frame automatically ensures an infinite order resummation in τ . Thus finally we get a series expansion of H_F in inverse drive-amplitude ($1/\gamma_k$) where all the terms are resummed in τ [59–62]. This extends the validity of H_F to the low drive frequency regime but limits it to the high drive amplitude regime.

The Hamiltonian for the driven system is given by,

$$H(t) = H_0 + H_D(t) \quad (S4)$$

where $H_0 = \sum_i (-1)^i S_i \cdot S_{i+1} - h \sum_i S_i^z$ and we apply a local drive at the k -th site $H_D(t) = \gamma_k \text{Sgn}(\sin(\omega t)) S_k^x$ with $\omega = 2\pi/\tau$. For open chains, we consider k to be a site in the bulk (e.g. the central site as was considered in the main text).

We now transform the time-dependent Hamiltonian to a rotating frame as follows,

$$H_{rot}(t) = W^\dagger H(t) W - iW^\dagger \partial_t W \quad (S5)$$

where

$$W(t) = e^{-i \int_0^t dt' H_D(t')} = e^{-i\theta(t) S_k^x} \quad (S6)$$

$\theta(t) = \gamma_k t \Theta(\tau/2 - t) + \gamma_k (\tau - t) \Theta(t - \tau/2)$. This transformation removes the driving term ($H_D(t)$) from the Hamiltonian in rotating frame ($H_{rot}(t)$) and we get

$$\begin{aligned} H_{rot}(t) &= W^\dagger H_0 W \\ &= \mathcal{H}(k-1, k) + \mathcal{H}(k, k+1) - h(\cos(\theta) S_k^z + \sin(\theta) S_k^y) + \sum_{\substack{i=1 \\ i \neq (k-1, k)}}^{N-1} (-1)^i S_i \cdot S_{i+1} - h \sum_{\substack{i=1 \\ i \neq k}}^N S_i^z \end{aligned} \quad (S7)$$

where $\mathcal{H}(k, k+1) = (-1)^k [S_k^x S_{k+1}^x + \cos(\theta)(S_k^y S_{k+1}^y + S_k^z S_{k+1}^z) - \sin(\theta)(S_k^z S_{k+1}^y - S_k^y S_{k+1}^z)]$ and we have used that $W^\dagger S_k^z W = \cos(\theta)S_k^z + \sin(\theta)S_k^y$ and $W^\dagger S_k^y W = -\sin(\theta)S_k^z + \cos(\theta)S_k^y$.

The stroboscopic Floquet Hamiltonian in F-M expansion is given by

$$H_F = \sum_{n=0}^{\infty} H_F^{(n)} \quad (\text{S8})$$

The zero-th order Floquet Hamiltonian is just the time averaged $H_{rot}(t)$ over one time period.

$$\begin{aligned} H_F^{(0)} &= \frac{1}{\tau} \int_0^\tau H_{rot}(t) dt \\ &= \mathcal{H}_F^{(0)}(k-1, k) + \mathcal{H}_F^{(0)}(k, k+1) + h_F^{(0)}(k) + \sum_{\substack{i=1 \\ i \neq (k-1, k)}}^{N-1} (-1)^i S_i \cdot S_{i+1} - h \sum_{\substack{i=1 \\ i \neq k}}^N S_i^z \end{aligned} \quad (\text{S9})$$

where

$$\begin{aligned} \mathcal{H}_F^{(0)}(k, k+1) &= (-1)^k [S_k^x S_{k+1}^x + \frac{2 \sin(\frac{\gamma_k \tau}{2})}{\gamma_k \tau} (S_k^y S_{k+1}^y + S_k^z S_{k+1}^z) - \frac{2(1 - \cos(\frac{\gamma_k \tau}{2}))}{\gamma_k \tau} (S_k^z S_{k+1}^y - S_k^y S_{k+1}^z)] \\ h_F^{(0)}(k) &= -\frac{2h}{\gamma_k \tau} [\sin(\frac{\gamma_k \tau}{2}) S_k^z + (1 - \cos(\frac{\gamma_k \tau}{2})) S_k^y] \end{aligned} \quad (\text{S10})$$
